行政院國家科學委員會專題研究計畫 成果報告

鎂合金薄板快速超塑性成形之特性研究
研究成果報告(精簡版)

計 畫 類 別 ：個別型
計 畫 編 號 ：NSC 98-2221-E-216-007-
執 行 期 間 ：98 年 08 月 01 日至 99 年 07 月 31 日
執 行 單 位 ：中華大學機械工程學系

計 畫 主 持 人：吳泓瑜

計畫參與人員：碩士班研究生-兼任助理人員：鄒明達
碩士班研究生-兼任助理人員：黃志超
大專生-兼任助理人員：林妗諭

處 理 方 式 ：本計畫可公開查詢

中 華 民 國 99 年 09 月 23 日

行政院國家科學委員會專題研究計畫成果報告

鎂合金薄板快速超塑性成形之特性研究

Characteristics of rapid gas blow forming of Mg alloy thin sheet

計畫編號：NSC 98-2221-E-216-007

執行期間：98年 8月 1日至99年 7月31日

計畫主持人: 吳泓瑜　　中華大學機械工程學系教授

E-mail: ncuwu@chu.edu.tw

計畫參與人員：黃志超、鄒明達、林妗諭 中華大學機械工程學系研究生

中文摘要

氣壓成形實驗中所使用為鎂合金AZ31B-O細晶板片，板片厚度為0.6mm，平均晶粒大小為5~6μm。藉此利用鎂合金AZ31B-O材在高溫下較佳的塑性變形能力以試圖減少成形所需的時間，也藉以了解快速氣壓成形的可行性，因此先採用300℃、370℃和420℃三種高溫溫度環境，在高溫環境下利用氣壓超塑性進行研究，探討多軸向應變狀態之氣壓成形特性。研究多軸向半球成形實驗中以階梯式加壓程序將成形時間控制為90秒及160秒內完成。探討AZ31B-O鎂合金在多軸應變狀態之變形過程中，試片半球成形性、厚度變化、極限延伸率及晶粒組織變化等情形；藉以分析得知溫度以及應變速率對成形參數之影響。結果表明，該加壓狀況對於成形時間的減少是可行的，並且當溫度越高則鎂合金高溫塑性能力提升，成形所需之最大壓力降低，本次實驗中370℃與420℃兩者成形性相近，且低應變速率加壓方式板片呈現較均勻的變形，同時420℃高溫環境下較容易靜態退火晶粒成長。

關鍵詞：AZ31B鎂合金、氣壓成形、加壓程序、自由鼓脹變形

Abstract

The deformation characteristics of a 0.6 mm-thick, fine-grained AZ31B Mg alloy sheet were investigated with the intention of reducing forming time during gas blow forming. The sheets were successfully deformed into the hemispherical domes at 300, 370, and 420ºC under various pressurization profiles. Results show that the proposed pressurization profiles could achieve the goal of reducing forming time. A stepwise pressurization profile may be a suitable process at lower temperatures; whereas, a constant or near constant pressure imposed during forming is a better method at higher temperatures. The pressurization profiles used in this study were not restricted to provide the optimum constant strain rate, which is always used in the traditional superplastic forming. Under the proposed pressurization profiles, maximum stress in the range of 23.5–45.6 MPa and resultant average strain rate in the

range of 6.63×10^{-3} to 1.56×10^{-2} s^{-1} were imposed on the deforming sheet at the apex of the dome. A more uniform distribution of the average strain rate along the centerline of the formed dome resulted in a bulged shape deviating from the perfect sphere shape as the deformation temperature increased.

Keywords: AZ31B Mg alloy; Gas blow forming; Pressurization profile; Free bulging.

1. Introduction

From the viewpoint of applied mechanics, one of the most important characteristics of superplastic materials is the high strain rate sensitivity of flow stress. The strain-rate sensitivity exponent, m (in the approximation of $\sigma = K\dot{\varepsilon}^m$), is the key in controlling the ductility of a superplastic material at elevated temperatures: the higher the value of m, the higher is the necking resistance. However, fine-grained superplastic materials exhibit high m-values only in a narrow range of strain rates, requiring careful process control to maintain the desired constant strain rate during superplastic forming (SPF). A significant problem in the commercial application of SPF on AZ31B alloy is low deformation rates (10^{-3}–10^{-4} s^{-1}) compared with other metal forming processes [1-4], which is undesirable in mass production.

Recently, to extend the industrial use of SPF, efforts have been devoted towards reducing forming times. As a result, quick plastic forming (QPF) technology has been developed [5-7]. The major difference between SPF and QPF lies in the deformation controlling mechanism. Superplasticity corresponds to deformation conditions in which grain boundary sliding (GBS) is the dominant controlling mechanism, with a value of m close to 0.5. However, the dislocation creep is expected to be the major deformation mechanism at higher strain rates and/or at lower temperatures [6,8,9], which are the deformation conditions for QPF. The dislocation creep produces medium strain-rate sensitivity (m ~ 0.33 to 0.2), although not as high as that of GBS creep. Moreover, it can provide sufficient tensile ductility [8,10,11]. QPF has been mainly studied in the case of Al alloys [9,12-15] and, to a much lesser extent, in the case of Mg alloys [8,16,17].

One of the authors recently examined the tensile flow behavior of a fine-grained AZ31B Mg alloy thin sheet and found an m-value of approximately 0.27 at a temperature of 370°C, with initial strain rates in the range of 4×10^{-3} to 1×10^{-1} s^{-1} [18]. This result implies that for a fine-grained AZ31B Mg alloy, the dislocation creep can be the controlling mechanism and QPF could be a possible gas blow forming process. In the present study, further, the deformation characteristics of a fine-grained AZ31B alloy were investigated using the stepwise pressurization profiles and constant pressure forming, with the intention of reducing forming time during gas blow forming. The effects of pressurization profiles on gas blow formability were studied. Results were quantitatively analyzed, and a detailed

description on the deformation behavior of an AZ31B alloy sheet is provided.

2. Experimental details

POSCO Company, Korea, provided the Mg alloy AZ31B-O thin sheet with a thickness of 0.6 mm used in this work. The analyzed chemical composition was (wt-%) Mg-3.01Al-0.98Zn-0.32Mn. The average grain size was approximately 5.4 μm before forming. The optical image of the original microstructure of the sheet is presented in Fig. 1.

Gas blow forming was carried out at temperatures of 300, 370 and 420°C using various pressurization profiles. Free bulging tests were performed by deforming the sheet into a right cylindrical die. The die cavity had an inner diameter of 40 mm with a die entry radius of 3.2 mm. Several interrupted tests were performed to deform the sheets to various degrees of heights for each pressurization profile.

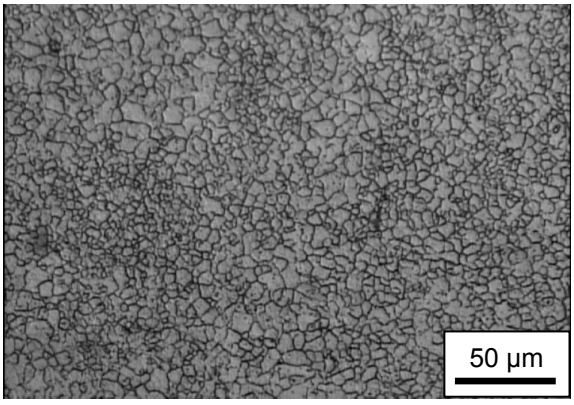

Fig. 1. Optical image of the microstructure of the fine- grained AZ31B Mg alloy.

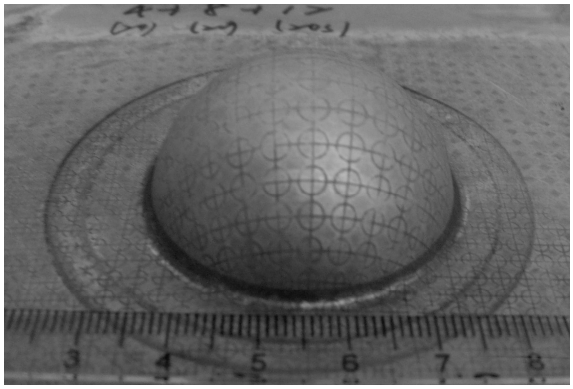

Fig. 2. A hemispherical dome formed by hot gas blow forming to demonstrate the deformed grid circles.

Grid circles of 2.5 mm in diameter were etched onto the sheets to measure the strain levels in each test. During forming the etched circles were distorted into ellipses and/or larger circles. The major and minor diameters of the deformed circles after deformation were measured to determine the principal strains, effective strains, and strain rates. Fig. 2 demonstrates the formed hemispherical dome to show the status of the deformed grid circles.

3. Results and discussion

3.1. Pressurization profile and formability

Free bulging tests were performed at various temperatures to explore the deformation characteristics according to the pressure-time profiles shown in Fig. 3. The terms PT300, PT370 and PT420 used in this study refer to the pressurization profiles for forming at 300, 370 and 420°C, respectively. There were two types of pressurization profiles proposed in this work. The first type included the pressurization profiles of PT300-160, PT370-75, PT370-150, and PT420-142, in which stepwise pressure increments were used during forming. The second type employed constant (PT420-83) and near constant (PT420-71) pressures during forming. Based on the resultant forming time and pressurization rate,

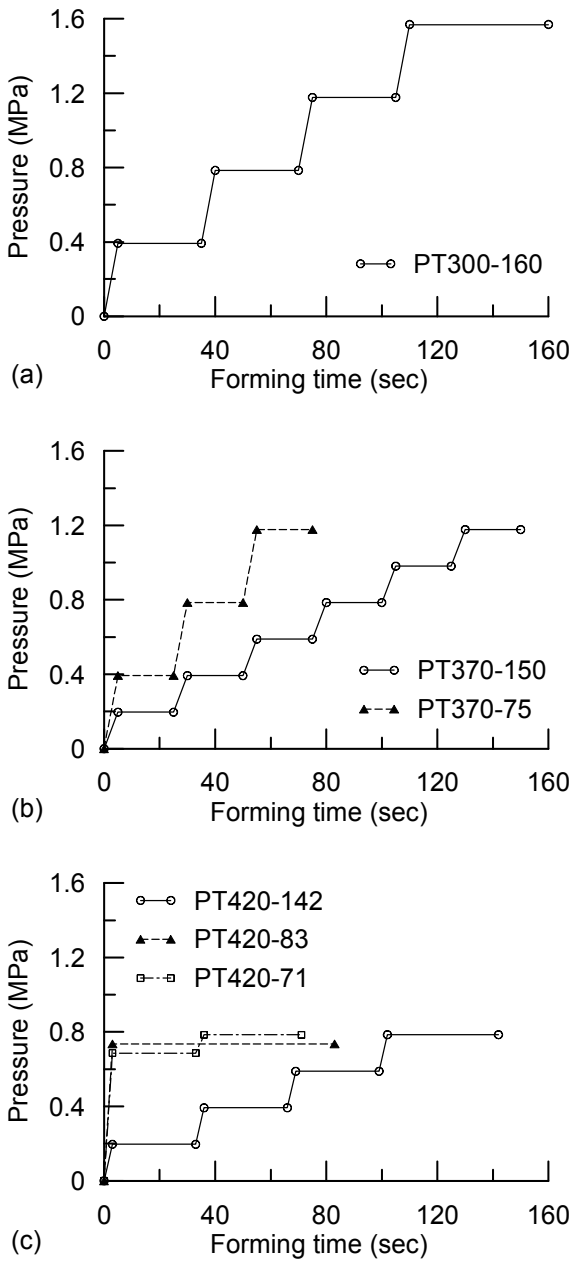

Fig. 3. Pressure-time profiles developed for hot gas blow forming: (a) at 300ºC, (b) at 370ºC, (c) at 420ºC.

PT300-160, PT370-150, and PT420-142 were classified as low pressurizing rate profiles. Meanwhile, PT370-75, PT420-71, and PT420-83 were classified as high pressurizing rate profiles.

The fine-grained AZ31B sheets were successfully formed into hemispherical domes at 300–420ºC following the pressurization profiles depicted in Fig.3. Although the dome could be formed at a temperature as low as 300ºC, it took a higher pressure and a longer time because the material had a higher flow stress. The final dome height revealed that forming at a low temperature of 300ºC would decrease formability. A lower pressure could be used to achieve a similar dome height at a higher temperature. The forming time could be significantly shortened using a profile with a higher pressurizing rate at the same temperature.

Constant pressures during forming were used to compare the deformation characteristics with those of the stepwise pressurization profiles. A constant pressure of 1.18 MPa for forming at 370ºC has been performed in this work. However, theforming failed at a dome height of approximately 16 mm. At a higher temperature of 420ºC, the sheet was successfully deformed into a hemispherical dome at a constant pressure of 0.74 MPa (PT420-83). Although the forming temperature of the pressurization profile PT370-75 is lower than that of PT420-83, using a stepwise pressure increment could reduce the forming time to achieve a similar dome height to that of PT420-83. This result indicates that a stepwise pressurization profile is likely to be a better process in reducing forming time at lower temperatures.

3.2. Deformation characteristics at the apex of the dome during forming

As the deformation proceeded, the proposed pressurization profiles did not

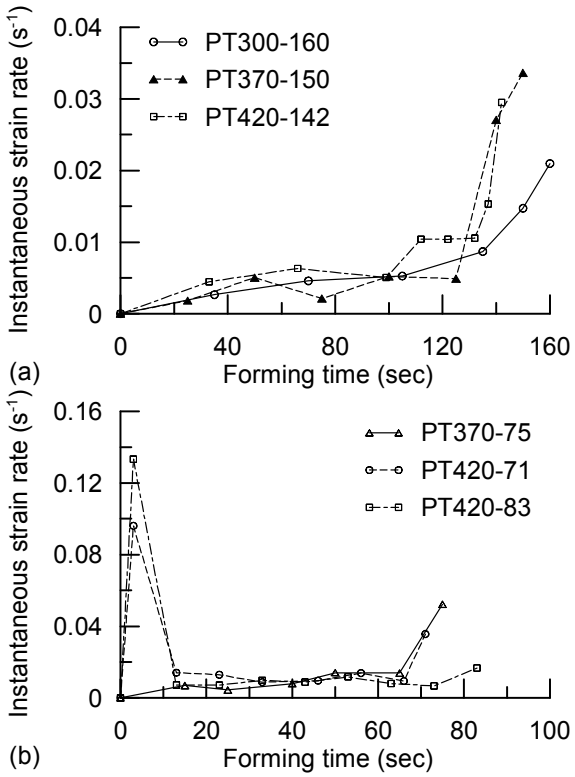

Fig. 4. Instantaneous strain rate at the dome apex as a function of forming time at various pressurization profiles: (a) at a low pressurizing rate profile, (b) at a high pressurizing rate profile.

provide constant strain rates during forming. The strain rate at the apex of the formed dome changed with forming time during deformation. Therefore, pressurization rate would influence the resultant forming time even at the same forming temperature with the same maximum pressure. The evolution of the instantaneous strain rate under various deformation conditions is given in Fig. 4. By measuring the thickness and diameters of the deformed grid circles, the instantaneous strain rate at the apex of the deformed sheet during forming can be calculated.

Similar instantaneous strain rate evolutions were observed for forming at low pressurizing rate profiles, as shown in Fig. 4a. The evolution of the instantaneous strain rate at the dome apex could be characterized by two distinctive regions for forming at a low pressurizing rate profile. Initially, the strain rate increased gradually for a certain period of forming time, and then increased rapidly at the end of forming. A similar instantaneous strain rate evolution was also observed for forming at the pressurization profile PT370-75, as shown in Fig. 4b. These results indicate that stepwise pressurization profiles would develop a similar evolution behavior of instantaneous strain rate at the apex during forming.

Relatively high initial strain rates observed for forming at PT420-83 and PT420-71 were due to relatively high pressures imposed at the beginning of forming, as illustrated in Fig. 4b. Subsequently, a rapid decrease in the strain rate was found, and this was followed by a near constant strain rate. The evolution behavior forming at PT420-83 (with constant pressure) is nearly the same as that forming at PT420-71 (with near constant pressure). However, a less significant increase in strain rate at PT420-83 was observed at the end of forming.

The evolution of the thickness at the dome apex as a function of forming time is illustrated in Fig. 5. The variation in thickness with forming time at the apex could be associated with the evolution of the instantaneous strain rate during forming. The behaviors of the thickness evolutions were very similar on testing at low pressurizing rate profiles, as shown in Fig. 5a. The thickness decreased gradually with increasing forming time. Rapid decreases in thickness arose at the end of forming at

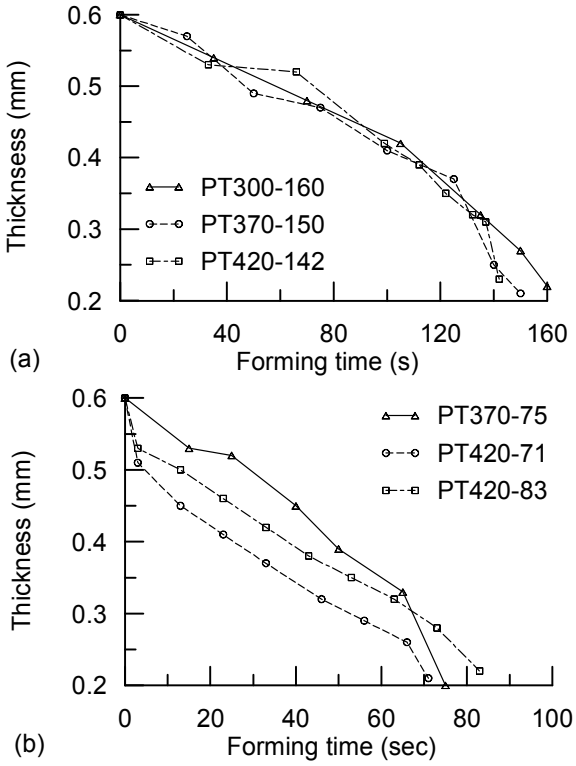

Fig. 5. Thickness at the dome apex as a function of forming time at various pressurization profiles: (a) at a low pressurizing rate profile, (b) at a high pressurizing rate profile.

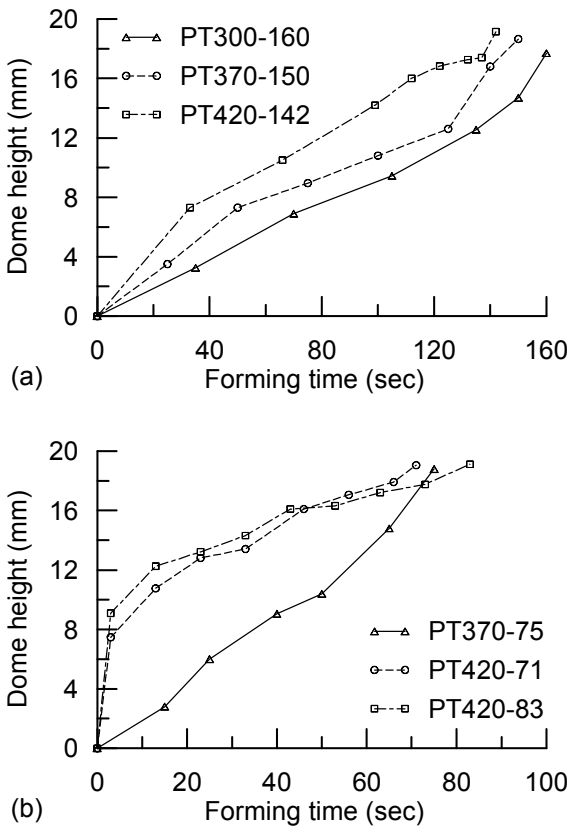

Fig. 6. Deformed dome apex height as a function of forming time at various pressurization profiles: (a) at a low pressurizing rate profile, (b) at a high pressurizing rate profile.

PT370-150 and PT420-142 when significant increases in instantaneous strain rates occurred. Fig. 5b reveals that the significant thinning at the apex observed at the beginning of forming is consistent with the relatively high instantaneous strain rate imposed for forming at PT420-71 and PT420-83. Rapid increases in the instantaneous strain rates at the end of forming also led to the significant decreases in thickness for forming at PT370-75 and PT420-71.

Deformation behavior is presented in Fig. 6 as a relationship between dome apex height and forming time. Two different evolution behaviors could be observed for forming at various pressurization profiles. Using a stepwise pressurization profile provides a nearly linear relationship of the dome height with forming time; whereas, forming with a constant or near constant pressurization profile exhibits a near power law relationship. Chung et al. [19] investigated the biaxial forming behavior of fine-grained AZ61 Mg alloy sheet using constant gas pressure and reported that the deformation process could be characterized by three distinctive regions. Initially, the height of the deforming dome increases rapidly, and an apparent steady state deformation stage is then reached. Finally, the deformation rate increases again as the

sheet is formed into a hemisphere. Fig. 6b indicates similar results for forming at PT420-71 and PT420-83, but no significant increase in the deformation rate was observed at the end of forming.

Considering that the forming sheet is part of hemispherical geometry having an instantaneous configuration and thickness as a function of time, using the equation for calculating the stress can justify the evolution behavior of the dome apex height. Based on the geometrical relationships proposed by Chung et al. [19] and Wittenauer et al. [20], the stress at the apex of the deformed sheet during gas blow forming can be calculated as

$$\sigma_{\text{gas}} = \frac{p_{gas} h}{t_0 \sin^2[2\tan^{-1}(h/r_0)]} \quad (1)$$

where σ_{gas} is the average stress (principal tangential stress along meridian line) acting at the apex of the hemispherical segment that has the deformed height of h; p_{gas} is the applied gas pressure; r_0 is the base radius of the dome; and t_0 is the initial thickness of the sheet. Fig. 7 displays the calculated stress as a function of forming time and shows that the stress increases continuously during forming under a profile of stepwise pressure increments, leading to a nearly linear relationship of the dome height with forming time. The constant or near constant pressure forming shows a high value of stress at the beginning of forming, resulting in a high deformation rate. Thereafter, a very gradual increase in the stress follows, causing a decrease in the deformation rate at the apex.

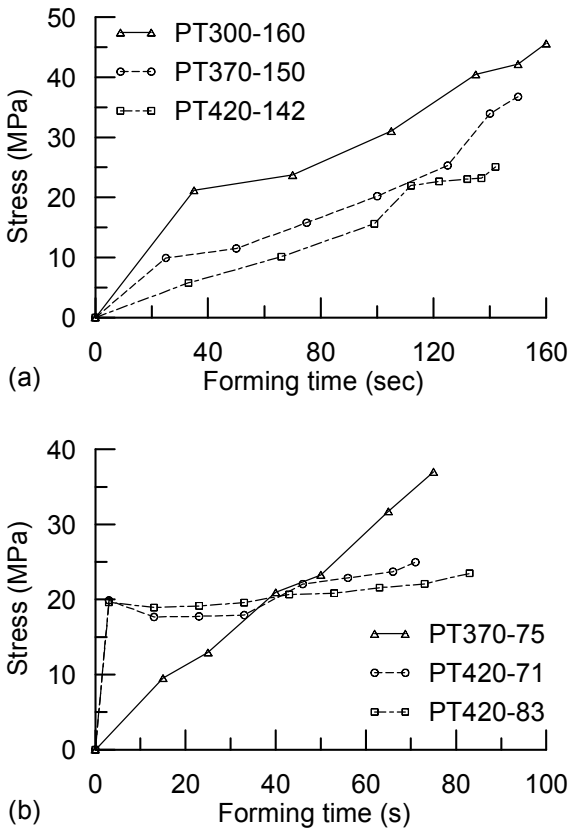

Fig. 7. Calculated stress at the apex of the formed dome as a function of forming time at various pressurization profiles: (a) at a low pressurizing rate profile, (b) at a high pressurizing rate profile.

3.4. Analyses of the bulge geometry

The average strain rate distribution along the centerline of the formed dome is given in Fig. 8. The average strain rate was calculated by dividing the final effective strain by the total forming time. The deformed grid circles and the thickness values of the last formed dome were measured to determine the final effective strains. A strain rate gradient exists for all proposed pressurization profiles, and the maximum strain rate occurs at the apex of the dome. During gas blow forming, the sheet deforms freely into a hemispherical segment. While a sheet clamped at the edge

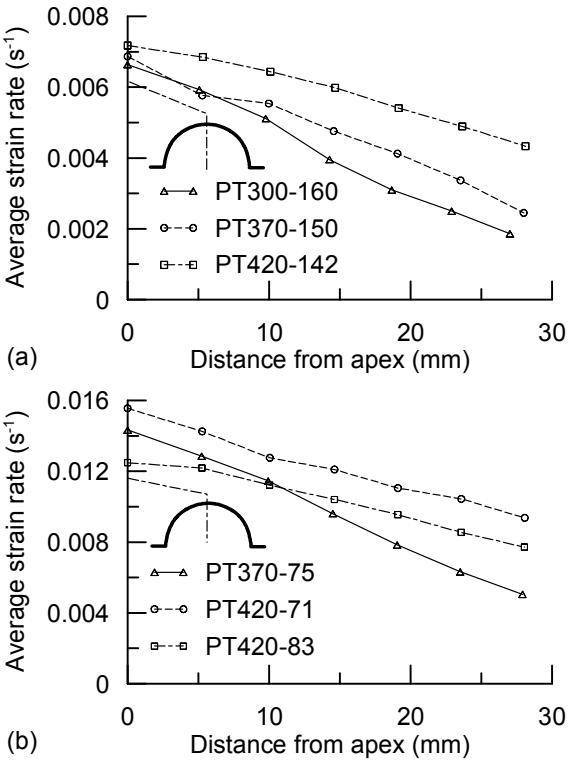

Fig. 8. Average strain rate distribution along the centerline of the dome formed at various pressurization profiles: (a) at a low pressurizing rate profile, (b) at a high pressurizing rate profile.

is subjected to a gas pressure to develop a part of the hemispherical geometry, the orthogonal stresses are equal at the apex, and the stress state is that of equi-biaxial tensile. At the edge of the dome, the constraint of the clamped sheet around the periphery results in a plane strain. A stress state gradient is evident from the apex of the dome to the edge in this geometry. The flow behavior of a fine-grained alloy sheet obeys the von Mises criterion [22]; hence, the apex experiences a higher stress than the edge, leading to a higher strain rate. The stress gradient in a forming dome causes a more rapid thinning at the apex, resulting in a strain rate gradient. Fig. 8 also shows that a more uniform distribution of the average strain rate was observed for forming at a higher temperature of 420ºC. A more uniform distribution of the average strain rate could lead to a more uniform deformation, reducing the gradient effect.

4. Conclusions

The deformation behaviors of a fine-grained AZ31B Mg alloy sheet were examined by gas pressure forming tests at temperatures of 300, 370, and 420ºC with various pressurization profiles in this work. Using the proposed pressurization profiles led to a non-constant strain rate deformation, which allowed the average strain rate at the apex in the order of 10^{-2} s^{-1} to be reached and the forming time to be reduced. The maximum average strain rates of 1.43×10^{-2} and 1.56×10^{-2} s^{-1} were achieved for forming at temperatures of 370 and 420°C, respectively. It was feasible to form a hemispherical dome with a height of approximately 19 mm in less than 85 s at a temperature higher than 370ºC. A higher pressurizing rate could significantly reduce the forming time for forming at the same temperature. Two distinctive regions in the variation in instantaneous strain rate with forming time were observed for forming under a stepwise pressurizing profile, while a relatively high strain rate was found at the beginning of deformation under a constant or near constant pressure forming. The thinning behavior at the dome apex could be associated with the variation in instantaneous strain rate with forming time, and the evolution of the dome height with forming time related to the stress developed at the apex.

References

[1] D.L. Yin, K.F. Zhang, G.F. Wang, W.B. Han, Mater. Letters 59 (2005) 1714–1718.

[2] J. C. Tan, M. J. Tan, Scripta Mater. 47 (2002) 101–106.

[3] F. K. Abu-Farha, M. K. Khraisheh, J. Mater. Eng. Perform. 16 (2007) 192–199.

[4] H. Watanabe, M. Fukusumi, Mater. Sci. Eng. A 477 (2008) 153–161.

[5] P.A. Friedman, W.B. Copple, J. Mater. Eng. Perform. 13 (2004) 335–347.

[6] P.E. Krajewski, J.G. Schroth, Overview of quick plastic forming technology, Materials Science Forum 551-552 (2007) 3–12.

[7] A.J. Barnes, J. Mater. Eng. Perform. 16 (2007) 440–454.

[8] R. Panicker, A.H. Chokshi, R.K. Mishra, R. Verma, P.E. Krajewski, Acta Mater. 57 (2009) 3683–3693.

[9] M.-A. Kulas, W.P. Green, E.M. Taleff, P.E. Krajewski, T.R. McNelley, Metall. Mater. Trans. A 36 (2005) 1249-1261.

[10] H. Watanabe, H. Tsutsui, Y. Mukai, M. Kohzu, S. Tanabe, K. Higashi, J. Plast. 17 (2001) 387–397.

[11] S.W. Chung, H. Watanabe, W.J. Kim, K. Higashi, Mater. Trans. 45 (2004) 1266–1271.

[12] P. Green, M.-A. Kulas, A. Niazi, K. Oishi, E.M. Taleff, P.E. Krajewski, T.R. McNelly, Metall. Mater. Trans. A 37 (2006) 2727-2738.

[13] E.M. Taleff, L.G. Hector Jr., J.R. Bradley, R. Verma, P.E. Krajewski, Acta Mater. 57 (2009) 2812–2822.

[14] M.-A. Kulas, P.E. Krajewski, J.R. Bradley, E.M. Taleff, Mater. Sci. Forum 551-552 (2007) 129–134.

[15] T.R. McNelley, K. Oh-ishi, A.P. Zhilyaev, S. Swaminathan, P.E. Krajewski, E.M. Taleff, Metall. Mater. Trans. A 39 (2008) 50–64.

[16] H. Somekawa, K. Hirai, H. Watanabe, Y. Takigawa, K. Higashi, Mater. Sci. Eng. A 407 (2005) 53–61.

[17] J.A. Del Valle, M.T. Perez-Prado, O.A. Ruano, Metall. Mater. Trans. A 36 (2005) 1427–1438.

[18] H.Y. Wu, W.C. Hsu, J. Alloys Compds 493 (2010) 590–594.

[19] S.W. Chung, K. Higashi, W.J. Kim, Mater. Sci. Eng. A 372 (2004) 15–20.

[20] J. Wittenauer, W.J. Kim, O.D. Sherby, Mater. Sci. Eng. A 194 (1994) 69–76.

[21] Y. Q. Song and J. Zhao, Mater. Sci. Eng. 84 (1986) 111–125.

[22] C. H. Hamiltom, Superplastic sheet forming, in: Superplasticity, AGARD Lecture Series No. 154, Specialised Printing Services limited, Loughton, Essex, 1987, pp. 2-1–2-23.

國科會補助專題研究計畫成果報告自評表

請就研究內容與原計畫相符程度、達成預期目標情況、研究成果之學術或應用價值（簡要敘述成果所代表之意義、價值、影響或進一步發展之可能性）、是否適合在學術期刊發表或申請專利、主要發現或其他有關價值等，作一綜合評估。

1. 請就研究內容與原計畫相符程度、達成預期目標情況作一綜合評估
   - ☑ 達成目標
   - ☐ 未達成目標（請說明，以 100 字為限）
     - ☐ 實驗失敗
     - ☐ 因故實驗中斷
     - ☐ 其他原因

   說明：

2. 研究成果在學術期刊發表或申請專利等情形：

   論文：☑已發表 ☐未發表之文稿 ☐撰寫中 ☐無

   專利：☐已獲得 ☐申請中 ☑無

   技轉：☐已技轉 ☑洽談中 ☐無

   其他：（以 100 字為限）

3. 請依學術成就、技術創新、社會影響等方面，評估研究成果之學術或應用價值（簡要敘述成果所代表之意義、價值、影響或進一步發展之可能性）（以 500 字為限）

   鎂合金快速超塑性成形技術的建立，對於未來推廣國內鎂板的應用具有重要的影響，有助於重建台灣鎂合金成形產業的榮景。鎂合金的快速氣壓成形，尤其是動態再結晶的超塑性成形研究，目前國內外均未見到相關學術論文發表。就學術觀點而言，本研究計畫的成果，已撰寫學術論文發表於國外 SCI 等級的著名學術期刊。鎂合金快速超塑性成形技術的開發，對國內 3C 產業將會有非常大的實質效益。由於鎂合金是輕量化不可或缺的材料，在運輸產業之應用會有更加顯著的效果，載具的輕量化使能源耗損少及降低二氧化碳之排放量，有節能與環保雙重意義。

無研發成果推廣資料

98 年度專題研究計畫研究成果彙整表

計畫主持人：吳泓瑜	計畫編號：98-2221-E-216-007-
計畫名稱：鎂合金薄板快速超塑性成形之特性研究	

成果項目			量化			單位	備註（質化說明：如數個計畫共同成果、成果列為該期刊之封面故事...等）
			實際已達成數（被接受或已發表）	預期總達成數(含實際已達成數)	本計畫實際貢獻百分比		
國內	論文著作	期刊論文	0	0	100%	篇	
		研究報告/技術報告	1	1	100%		
		研討會論文	2	2	100%		
		專書	0	0	100%		
	專利	申請中件數	0	0	100%	件	
		已獲得件數	0	0	100%		
	技術移轉	件數	0	0	100%	件	
		權利金	0	0	100%	千元	
	參與計畫人力（本國籍）	碩士生	2	2	100%	人次	
		博士生	0	0	100%		
		博士後研究員	0	0	100%		
		專任助理	0	0	100%		
國外	論文著作	期刊論文	1	1	100%	篇	
		研究報告/技術報告	0	0	100%		
		研討會論文	1	1	100%		
		專書	0	0	100%	章/本	
	專利	申請中件數	0	0	100%	件	
		已獲得件數	0	0	100%		
	技術移轉	件數	0	0	100%	件	
		權利金	0	0	100%	千元	
	參與計畫人力（外國籍）	碩士生	0	0	100%	人次	
		博士生	0	0	100%		
		博士後研究員	0	0	100%		
		專任助理	0	0	100%		

其他成果 (無法以量化表達之成果如辦理學術活動、獲得獎項、重要國際合作、研究成果國際影響力及其他協助產業技術發展之具體效益事項等，請以文字敘述填列。)	無

	成果項目	量化	名稱或內容性質簡述
科教處計畫加填項目	測驗工具(含質性與量性)	0	
	課程/模組	0	
	電腦及網路系統或工具	0	
	教材	0	
	舉辦之活動/競賽	0	
	研討會/工作坊	0	
	電子報、網站	0	
	計畫成果推廣之參與（閱聽）人數	0	

國科會補助專題研究計畫成果報告自評表

請就研究內容與原計畫相符程度、達成預期目標情況、研究成果之學術或應用價值（簡要敘述成果所代表之意義、價值、影響或進一步發展之可能性）、是否適合在學術期刊發表或申請專利、主要發現或其他有關價值等，作一綜合評估。

1. 請就研究內容與原計畫相符程度、達成預期目標情況作一綜合評估

■達成目標

□未達成目標（請說明，以 100 字為限）

□實驗失敗

□因故實驗中斷

□其他原因

說明：

2. 研究成果在學術期刊發表或申請專利等情形：

論文：■已發表 □未發表之文稿 □撰寫中 □無

專利：□已獲得 □申請中 ■無

技轉：□已技轉 ■洽談中 □無

其他：(以 100 字為限)

3. 請依學術成就、技術創新、社會影響等方面，評估研究成果之學術或應用價值（簡要敘述成果所代表之意義、價值、影響或進一步發展之可能性）(以 500 字為限)

鎂合金快速超塑性成形技術的建立，對於未來推廣國內鎂板的應用具有重要的影響，有助於重建台灣鎂合金成形產業的榮景。鎂合金的快速氣壓成形，尤其是動態再結晶的超塑性成形研究，目前國內外均未見到相關學術論文發表。就學術觀點而言，本研究計畫的成果，已撰寫學術論文發表於國外 SCI 等級的著名學術期刊。鎂合金快速超塑性成形技術的開發，對國內 3C 產業將會有非常大的實質效益。由於鎂合金是輕量化不可或缺的材料，在運輸產業之應用會有更加顯著的效果，載具的輕量化使能源耗損少及降低二氧化碳之排放量，有節能與環保雙重意義。